HHS Public Access

Author manuscript

Clin Cancer Res. Author manuscript; available in PMC 2022 June 03.

Published in final edited form as:

Clin Cancer Res. 2019 April 01; 25(7): 2064–2071. doi:10.1158/1078-0432.CCR-18-3133.

Immunologic correlates of the abscopal effect in a SMARCB1/INI1-negative Poorly Differentiated Chordoma after EZH2 inhibition and radiotherapy

Mrinal Gounder[1,*], **Guo Zhu**[2,*], **Lev Roshal**[2], **Eric Lis**[1], **Scott Daigle**[3], **Steven Blakemore**[3], **Neil Michaud**[3], **Meera Hameed**[2], **Travis J. Hollmann**[2]

[1]Developmental Therapeutics Service, Memorial Sloan Kettering Cancer Center and Weil Cornell Medical School, New York, NY;

[2]Department of Pathology, Memorial Sloan Kettering Cancer Center;

[3]Epizyme, Cambridge, MA.

Abstract

Purpose: We sought to determine the mechanism of an exceptional response in a patient diagnosed with a SMARCB1/INI1-negative chordoma treated with tazemetostat, an EZH2 inhibitor and followed by radiotherapy.

Experimental Design: In an attempt to investigate the mechanism behind this apparent abscopal effect, we interrogated tumor tissues obtained over the clinical course. We utilized next-generation sequencing, standard IHC and employed a novel methodology of multiplex immunofluorescence analysis

Results: We report an exceptional and durable response (2+ years) in a patient with SMARCB1 deleted, metastatic, poorly differentiated chordoma; a lethal disease with an overall survival of 6 months. The patient was treated for 4 weeks with tazemetostat, an EZH2 inhibitor in a phase II clinical trial. At the time of progression she underwent radiation to the primary site and unexpectedly had a complete response at distant metastatic sites. We evaluated baseline and on-treatment tumor biopsies and demonstrate that tazemetostat resulted in pharmacodynamic inhibition of EZH2 as seen by decrease in histone methylation at H3K27me3. Tazemetostat resulted in a significant increase in intratumoral and stromal infiltration by proliferative (high Ki-67), CD8+ T cells, FOxP3+ regulatory T cells and immune cells expressing checkpoint regulators PD-1 and LAG-3. These changes were pronounced in the stroma.

Conclusions: These observations are the first demonstration in patient samples confirming that EZH2 inhibition can promote a sustained antitumor response that ultimately leads to T cell exhaustion and checkpoint activation. This suggests that targeted altering of the epigenetic landscape may sensitize some tumors to checkpoint inhibitors

Corresponding author: Mrinal Gounder, M.D., Developmental Therapeutics Service, Memorial Sloan-Kettering Cancer Center, 300 E 66th St BAIC 1075, New York, NY 10065, 646-888-4167 phone/ 646-888-4252 fax, gounderm@mskcc.org.

*These authors contributed equally to this article

Keywords

EZH2; tazemetostat; tumor microenvironment; epigenetics; chordoma; checkpoint blockade

Introduction:

Chordoma is a rare cancer of the spine with an annual incidence of approximately 300 new cases in the United States. It can occur at any age and presents as a localized mass causing pain and neurological symptoms. For conventional chordoma (>95%) surgery and/or radiotherapy (RT) are considered standard of care, however 10-year disease-specific survival is ~48% (1). In contrast, poorly differentiated chordoma (PDC) (2), is highly aggressive, often metastatic and uniformly fatal with a median overall survival of 9 months (3–5). Unlike conventional chordoma, PDC can be sensitive to cytotoxic chemotherapies; however the responses are short-lived.

SMARCB1 (INI1) is a critical component of the mammalian SWItch/Sucrose Non-Fermentable (mSWI/SNF) protein complex which is essential for chromatin remodeling and in some cellular contexts can function as a tumor suppressor or oncogene. TCGA analysis shows that ~20% of all cancers harbor inactivating mutations in the mSWI/SNF complex (6). Loss of tumor suppression through *SMARCB1/INI1* inactivation has been described as a key genetic event in various tumor types (7), including malignant rhabdoid tumors (MRT) and epithelioid sarcoma. Therefore, targeting cancers with dysfunctional mSWI/SNF complexes is an area of active interest.

Loss of the SMARCB1/INI1 subunit destabilizes the mSWI/SNF complex, resulting in unopposed oncogenic activity of Enhancer of Zeste homolog 2 (EZH2) (8,9), a histone methyltransferase. EZH2 functions as an epigenetic regulator of gene expression by catalyzing the generation of trimethylated H3K27 (H3K27me3), which results in the repression of broad transcriptional gene sets thereby regulating cellular differentiation programs. Inhibition of EZH2 confers synthetic lethality in SMARCB1/INI1 deficient tumors. In a Phase 1 study of tazemetostat, an oral inhibitor of EZH2, complete and partial responses (RECIST 1.1) were seen in patients with SMARCB1/INI1-negative tumors (10).

In pre-clinical studies, EZH2 has been implicated in affecting the tumor microenvironment through several mechanisms involving multiple immune cell types (11,12). In this case report, we sought to determine the mechanism of an exceptional and durable response in a patient diagnosed with a SMARCB1/INI1-negative PDC treated with tazemetostat and sequential radiotherapy. Here, we demonstrate the first comprehensive in-patient evidence for a potential link between inhibition of EZH2 and its impact on tumor immunology.

Clinical Summary

A 25-year-old female presented with lower back pain, bowel and bladder dysfunction and lower extremity paresthesia. Spinal MRI scan showed a 6.4 cm sacral mass and staging studies showed loco-regional spread and lung metastasis (Figure 1A). A biopsy of the primary sacral mass confirmed poorly differentiated chordoma with SMARCB1/INI1 loss

by IHC (labelled: “Baseline, Sacrum”) (Fig 2A–C). Next-generation sequencing of the tumor confirmed an intragenic deletion of exons 5–7 and loss of heterozygosity of the *SMARCB1* on chromosome 22 and very low tumor mutation burden.

The patient signed informed consent form (MSKCC IRB#15–328) to a Phase 2 study of tazemetostat in SMARCB1/INI1-negative tumors (Clinicaltrials.gov NCT02601937) and additionally consented to optional tumor biopsies. The trial was conducted in accordance with the Declaration of Helsinki, Good Clinical Practice guidelines, and federal and local policy on bioethics and human biologic specimens. At enrollment, imaging scans showed rapid growth in the sacral primary and metastatic pulmonary nodules (Figure 1B). After 4 weeks of tazemetostat treatment (800 mg, oral, twice daily) the patient noted worsening symptoms and withdrew from study although imaging revealed stable disease by RECIST 1.1 (+13%) (Figure 1C). An on-study biopsy of the sacral mass (labelled “On-Tazemetostat, Sacrum”) was performed. The patient underwent radiation to the primary sacral mass (7000 cGy over 35 fractions) which resulted in a partial response in the radiated sacrum and a complete response in the distant, metastatic lung nodules (non-radiated) (Figure 1D). A durable complete response was observed for four months when follow up imaging revealed bilateral recurrent disease in the lung (Figure 1E). The largest metastatic nodule was incompletely removed (labelled “Taz → sacral RT, Lung). Given the initial abscopal effect observed on tazemetostat and sequential RT, the patient was treated with off-label, nivolumab, a PD-1 inhibitor. Following 6 cycles of nivolumab, all lung nodules disappeared; however, the primary sacral (post-radiated) chordoma remained resistant (Figure 1F). The patient subsequently received additional radiation to the sacrum (3000 cGy, 5 fractions) with tumor shrinkage. Following a second radiation, the CTLA-4 inhibitor ipilumimab (1 mg/kg q21 days x 4 doses) was added to nivolumab; however the primary sacral site remained unresponsive to immunotherapy while the metastatic lung lesions are in complete remission for 2+ years.

In an attempt to investigate the mechanism behind this apparent abscopal effect, we interrogated tumor tissues obtained over the clinical course. We utilized standard IHC and employed a novel methodology of multiplex immunofluorescence analysis.

RESULTS

Modulation of the tumor immune microenvironment by sequential EZH2 inhibition and radiation therapy (RT)

The treatment-naïve sacral PDC tumor displayed strong, diffuse H3K27me3 IHC staining (Figure 2D) and treatment with tazemetostat demonstrated a dramatic decrease in H3K27me3 staining, pharmacodynamic evidence of EZH2 inhibition confirming the molecular action of tazemetostat (Figure 2E). While there was minimal immune cell infiltration of the primary untreated tumor, tazemetostat treated tumor showed an increase in intratumoral and stromal infiltration by CD8+ cytotoxic T lymphocytes (CTLs), FoxP3+ regulatory T cells (Tregs), and immune cells expressing checkpoint regulators PD-1 and LAG-3 (Figure 2F, 2G and 3A,B). Tazemetostat induced increases in CD8+ T cell subtypes with singular or combined expression of T cell exhaustion markers PD-1 and LAG-3, changes that were more pronounced in the stroma as might be expected for T cells showing

expression of so-called “exhaustion” markers with some impairment of infiltration into tumor (Figure 3B).

Prior to tazemetostat treatment, virtually all of tumor-infiltrating CD8+ CTLs were nonproliferative (>98% Ki67-negative). The number and percentage of Ki-67-positive CD8+ CTLs increased significantly in both the intratumoral and stromal compartments with tazemetostat therapy (Figure 2F, 2G and 3C). A significant percentage of selected CD8+ CTL subtypes demonstrated staining of the proliferation marker Ki-67, most notably LAG-3+ stromal CTLs (Figure 3C). The increased number of T cells, and shift towards more proliferative T lymphocytes with concomitant expression of checkpoint markers indicates a shift in the immune status of the tumor upon tazemetostat treatment consistent with activation of a antitumor immune response and emergence of CD8+ T cell exhaustion. These observations are the first demonstration in patient samples confirming that EZH2 inhibition can promote a sustained antitumor response that ultimately leads to T cell exhaustion defined by expression of inhibitory checkpoint expression.

Examination of the largest, recurrent lung lesion (Taz → sacral RT, Lung) that emerged after the abscopal effect seen with sequential tazemetostat and radiation revealed the presence of infiltrating immune cells, including CD8+ CTLs, FoxP3+ Tregs, and PD-1+, PD-L1+ and LAG-3+ immune cells (Figure 2H,I). Increased intratumoral density of CD8+ T cell subtypes compared to the primary sacral PDC tumor was detected but stromal infiltration was much more robust (Figure 3A and 3B). As seen with tazemetostat treatment, elevated numbers of proliferative stromal CTLs were observed compared to the primary PDC (Figure 3C). Multiple intratumoral and stromal CD8+ CTL subpopulations were Ki-67+ following RT, and stromal PD-1+ CTL subtypes with proliferative potential were generally the most abundant (Figure 3C). It is not possible to ascertain from these data what contribution each therapy made to the systemic immune response that resulted in T cell infiltration of the metastatic lung tumors. More studies are needed to determine the individual and combined effect of tazemetostat and RT to this phenomenon. Interestingly, the presence of PD-L1+ immune cells (Figure 2I) in the resected lung nodule indicates immune checkpoint engagement and dampening of the antitumor immune response, which may have contributed to recurrence of some lung lesions following RT. Further, the presence of proliferative (Ki-67+) CD8+ CTL subtypes at the metastatic tumor site may explain the impressive responses of the lung lesions to single agent nivolumab.

DISCUSSION

In this case report, we provide evidence that EZH2 blockade with tazemetostat can induce can antitumor immune response by promoting tumor infiltration by various T cell populations, further demonstrating the potential impact of epigenetic regulation of immunological responses in cancer. The patient described in this report is now alive at 27+ months following diagnosis and continues to have a complete response in the metastatic sites. This represents an exceptional response in this otherwise lethal disease with a median overall survival of 9 months

EZH2 and its role in tumor microenvironment

EZH2 function impairs antigen presentation through inhibiting MHC class I and II gene expression(13,14) interferes with expression of cytokines, their receptors and the IFN-γ transcriptional program,(15) promotes maintenance of Treg cell identity and immunosuppressive function (11,12,16), attenuates trafficking of effector CD8+ T cells through repression of chemokines CXCL9 and CXCL10, and impairs maturation of NK cells (17). Preclinically, increased EZH2 is implicated in resistance to anti-CTLA4 immunotherapy through diminished antigen presentation, which is subsequently overcome by EZH2 inhibition leading to PD-L1 downregulation and infiltration of IFN-γ-producing PD-1^{low} $CD8^{+}$ T cells (18).

Tazemetostat treatment appears to have induced an antitumor response in the primary PDC based on modulation of the tumor immune microenvironment in multiple ways. In our study, we observed substantial tumor infiltration by various lymphocytes, including proliferative CD8+ T cells, following EZH2 inhibition with tazemetostat alone. Based on many published observations that increased intratumoral infiltrating lymphocyte density, most notably CD8 positive cells, correlates with improved survival in many tumors, we quantitatively reported intratumoral and stromal densities for the multiplex panel marker expression providing spatial contexture to CD8 cell infiltration and co-expression. Tazemetostat may have induced lymphocyte infiltration of the PCD through reported effects of EZH2 disruption on reprogramming of tumor infiltrating Tregs to stimulate T cell infiltration (11,12,17) or by upregulating chemokine and cytokine expression (15,19). Further evidence of an antitumor immune response in the primary PDC induced by tazemetostat is apparent from the detection of T cell exhaustion, as evidenced by the expression of inhibitory immune checkpoint receptors PD-1 and LAG-3 either singularly or in combination on CD8+ T cells found both intratumorally and within the stroma (Figure 3B). Induced expression of these exhaustion markers is indicative of prolonged exposure of T cells to their cognate antigen that is associated with decreased proliferation and loss of T cell effector functions after an initial immune response (20). Generally co-upregulation of multiple inhibitory receptors indicates a higher degree of T cell dysfunction (21). Nonetheless, further studies are needed to investigate the involvement of these mechanisms in the phenotypic effects of EZH2 inhibition in the immune microenvironment of human tumors.

The primary, heavily radiated, recurrent sacral mass was refractory to immune checkpoint blockade (ICB) administered well after tazemetostat therapy. We hypothesize that increased levels of exhausted intratumoral and stromal CD8+ CTLs, as evidenced by PD-1 and LAG-3 expression on these cells in the primary PDC (Figure 3B), may explain the attenuated response of the primary tumor to tazemetostat despite the presence of proliferation competent CD8+ CTLs in the tumor. Concurrent treatment of the primary PDC with tazemetostat and an immune checkpoint inhibitor such as nivolumab may have been required to reverse T cell exhaustion and reinvigorate infiltrating T cells to effect tumor shrinkage. However, the dual expression of PD-1 and LAG-3 on exhausted T cells in the sacral PDC may have precluded an objective response to combination tazemetostat / ICB treatment. Additionally, gene expression profiling of PDC tumors from patients treated with tazemetostat, RT or ICBs to investigate the molecular profiles of T cell exhaustion may

provide future insights into sensitivity and resistance to these agents. Finally, we hypothesize that RT of the sacrum likely depleted the TILs induced by tazemetostat at the primary site, thus making the sacral mass refractory to immunotherapy.

The complete response of the metastatic lung tumors following RT of the primary PDC conforms to the classical definition of the abscopal effect of radiotherapy that results in tumor regression at non-irradiated, distant sites. This phenomenon is extremely rare. The precise mechanisms underlying abscopal responses remain unclear, but emerging evidence suggests systemic activation of the immune system is the basis for this response (22). It is thought that RT induces immunogenic cell death, characterized by release of danger-associated molecular pattern (DAMP) antigens that then trigger antigen uptake and activation of antigen presenting cells leading to subsequent priming of cytotoxic T lymphocytes and an adaptive immune response.

Tazemetostat clearly stimulated an antitumor immune response within the primary PDC, and robust immune infiltration of the distant lung tumor was detected following RT. Nonetheless, it is difficult to discern the exact contribution of EZH2 inhibition, RT and PD-1 blockade on the immunological and overall responses of the patient. To further discern the contribution of each of these therapies, it will be important to study sequential biopsies from both primary and recurrent sacral and metastatic tumors, as well as peripheral blood samples to evaluate systemic immunological changes with each intervention in future clinical studies. These additional samples will also help elucidate the role of tumor mutation burden/neoantigen load, T cell receptor repertoire and expansion of specific T cell clones in immunological and therapeutic responses to EZH2 inhibition and RT.

In conclusion, we convincingly demonstrate for the first time in a patient that EZH2 inhibition with tazemetostat induces an immune response within the tumor microenvironment. Following tazemetostat treatment, sequential RT and checkpoint blockade led to an exceptional response in this patient. Further studies are warranted to elucidate the contribution of each therapy to TME remodeling and therapeutic response. Importantly, the favorable tolerability and safety of tazemetostat makes it a promising drug to conduct investigational combination studies with radiation and/or checkpoint inhibitors.

Supplementary Material

Refer to Web version on PubMed Central for supplementary material.

References

1. Smoll NR, Gautschi OP, Radovanovic I, Schaller K, Weber DC. Incidence and relative survival of chordomas: the standardized mortality ratio and the impact of chordomas on a population. Cancer 2013;119(11):2029–37 doi 10.1002/cncr.28032. [PubMed: 23504991]
2. Shih AR, Cote GM, Chebib I, Choy E, DeLaney T, Deshpande V, et al. Clinicopathologic characteristics of poorly differentiated chordoma. Mod Pathol 2018 doi 10.1038/s41379-018-0002-1.
3. Chavez JA, Nasir Ud D, Memon A, Perry A. Anaplastic chordoma with loss of INI1 and brachyury expression in a 2-year-old girl. Clin Neuropathol 2014;33(6):418–20 doi 10.5414/NP300724. [PubMed: 25074874]

4. Hasselblatt M, Thomas C, Hovestadt V, Schrimpf D, Johann P, Bens S, et al. Poorly differentiated chordoma with SMARCB1/INI1 loss: a distinct molecular entity with dismal prognosis. Acta Neuropathol 2016;132(1):149–51 doi 10.1007/s00401-016-1574-9. [PubMed: 27067307]
5. Mobley BC, McKenney JK, Bangs CD, Callahan K, Yeom KW, Schneppenheim R, et al. Loss of SMARCB1/INI1 expression in poorly differentiated chordomas. Acta Neuropathol 2010;120(6):745–53 doi 10.1007/s00401-010-0767-x. [PubMed: 21057957]
6. Kadoch C, Crabtree GR. Mammalian SWI/SNF chromatin remodeling complexes and cancer: Mechanistic insights gained from human genomics. Sci Adv 2015;1(5):e1500447 doi 10.1126/sciadv.1500447. [PubMed: 26601204]
7. Hollmann TJ, Hornick JL. INI1-deficient tumors: diagnostic features and molecular genetics. Am J Surg Pathol 2011;35(10):e47–63 doi 10.1097/PAS.0b013e31822b325b. [PubMed: 21934399]
8. Knutson SK, Warholic NM, Wigle TJ, Klaus CR, Allain CJ, Raimondi A, et al. Durable tumor regression in genetically altered malignant rhabdoid tumors by inhibition of methyltransferase EZH2. Proc Natl Acad Sci U S A 2013;110(19):7922–7 doi 10.1073/pnas.1303800110. [PubMed: 23620515]
9. Wilson BG, Wang X, Shen X, McKenna ES, Lemieux ME, Cho YJ, et al. Epigenetic antagonism between polycomb and SWI/SNF complexes during oncogenic transformation. Cancer Cell 2010;18(4):316–28 doi 10.1016/j.ccr.2010.09.006. [PubMed: 20951942]
10. Italiano A, Soria JC, Toulmonde M, Michot JM, Lucchesi C, Varga A, et al. Tazemetostat, an EZH2 inhibitor, in relapsed or refractory B-cell non-Hodgkin lymphoma and advanced solid tumours: a first-in-human, open-label, phase 1 study. Lancet Oncol 2018;19(5):649–59 doi 10.1016/S1470-2045(18)30145-1. [PubMed: 29650362]
11. Goswami S, Apostolou I, Zhang J, Skepner J, Anandhan S, Zhang X, et al. Modulation of EZH2 expression in T cells improves efficacy of anti-CTLA-4 therapy. J Clin Invest 2018 doi 10.1172/JCI99760.
12. Wang D, Quiros J, Mahuron K, Pai CC, Ranzani V, Young A, et al. Targeting EZH2 Reprograms Intratumoral Regulatory T Cells to Enhance Cancer Immunity. Cell Rep 2018;23(11):3262–74 doi 10.1016/j.celrep.2018.05.050. [PubMed: 29898397]
13. Abou El Hassan M, Yu T, Song L, Bremner R. Polycomb Repressive Complex 2 Confers BRG1 Dependency on the CIITA Locus. J Immunol 2015;194(10):5007–13 doi 10.4049/jimmunol.1403247. [PubMed: 25862816]
14. Truax AD, Thakkar M, Greer SF. Dysregulated recruitment of the histone methyltransferase EZH2 to the class II transactivator (CIITA) promoter IV in breast cancer cells. PLoS One 2012;7(4):e36013 doi 10.1371/journal.pone.0036013. [PubMed: 22563434]
15. Abou El Hassan M, Huang K, Eswara MB, Zhao M, Song L, Yu T, et al. Cancer Cells Hijack PRC2 to Modify Multiple Cytokine Pathways. PLoS One 2015;10(6):e0126466 doi 10.1371/journal.pone.0126466. [PubMed: 26030458]
16. DuPage M, Chopra G, Quiros J, Rosenthal WL, Morar MM, Holohan D, et al. The chromatin-modifying enzyme Ezh2 is critical for the maintenance of regulatory T cell identity after activation. Immunity 2015;42(2):227–38 doi 10.1016/j.immuni.2015.01.007. [PubMed: 25680271]
17. Yin J, Leavenworth JW, Li Y, Luo Q, Xie H, Liu X, et al. Ezh2 regulates differentiation and function of natural killer cells through histone methyltransferase activity. Proc Natl Acad Sci U S A 2015;112(52):15988–93 doi 10.1073/pnas.1521740112. [PubMed: 26668377]
18. Zingg D, Arenas-Ramirez N, Sahin D, Rosalia RA, Antunes AT, Haeusel J, et al. The Histone Methyltransferase Ezh2 Controls Mechanisms of Adaptive Resistance to Tumor Immunotherapy. Cell Rep 2017;20(4):854–67 doi 10.1016/j.celrep.2017.07.007. [PubMed: 28746871]
19. Peng D, Kryczek I, Nagarsheth N, Zhao L, Wei S, Wang W, et al. Epigenetic silencing of TH1-type chemokines shapes tumour immunity and immunotherapy. Nature 2015;527(7577):249–53 doi 10.1038/nature15520. [PubMed: 26503055]
20. Thommen DS, Schumacher TN. T Cell Dysfunction in Cancer. Cancer Cell 2018;33(4):547–62 doi 10.1016/j.ccell.2018.03.012. [PubMed: 29634943]
21. Zarour HM. Reversing T-cell Dysfunction and Exhaustion in Cancer. Clin Cancer Res 2016;22(8):1856–64 doi 10.1158/1078-0432.CCR-15-1849. [PubMed: 27084739]

22. Abuodeh Y, Venkat P, Kim S. Systematic review of case reports on the abscopal effect. Curr Probl Cancer 2016;40(1):25–37 doi 10.1016/j.currproblcancer.2015.10.001. [PubMed: 26582738]

23. Bodenmiller B Multiplexed Epitope-Based Tissue Imaging for Discovery and Healthcare Applications. Cell Syst 2016;2(4):225–38 doi 10.1016/j.cels.2016.03.008. [PubMed: 27135535]

24. Stack EC, Wang C, Roman KA, Hoyt CC. Multiplexed immunohistochemistry, imaging, and quantitation: a review, with an assessment of Tyramide signal amplification, multispectral imaging and multiplex analysis. Methods 2014;70(1):46–58 doi 10.1016/j.ymeth.2014.08.016. [PubMed: 25242720]

25. Cheng DT, Mitchell TN, Zehir A, Shah RH, Benayed R, Syed A, et al. Memorial Sloan Kettering-Integrated Mutation Profiling of Actionable Cancer Targets (MSK-IMPACT): A Hybridization Capture-Based Next-Generation Sequencing Clinical Assay for Solid Tumor Molecular Oncology. J Mol Diagn 2015;17(3):251–64 doi 10.1016/j.jmoldx.2014.12.006. [PubMed: 25801821]

26. Zehir A, Benayed R, Shah RH, Syed A, Middha S, Kim HR, et al. Mutational landscape of metastatic cancer revealed from prospective clinical sequencing of 10,000 patients. Nat Med 2017;23(6):703–13 doi 10.1038/nm.4333. [PubMed: 28481359]

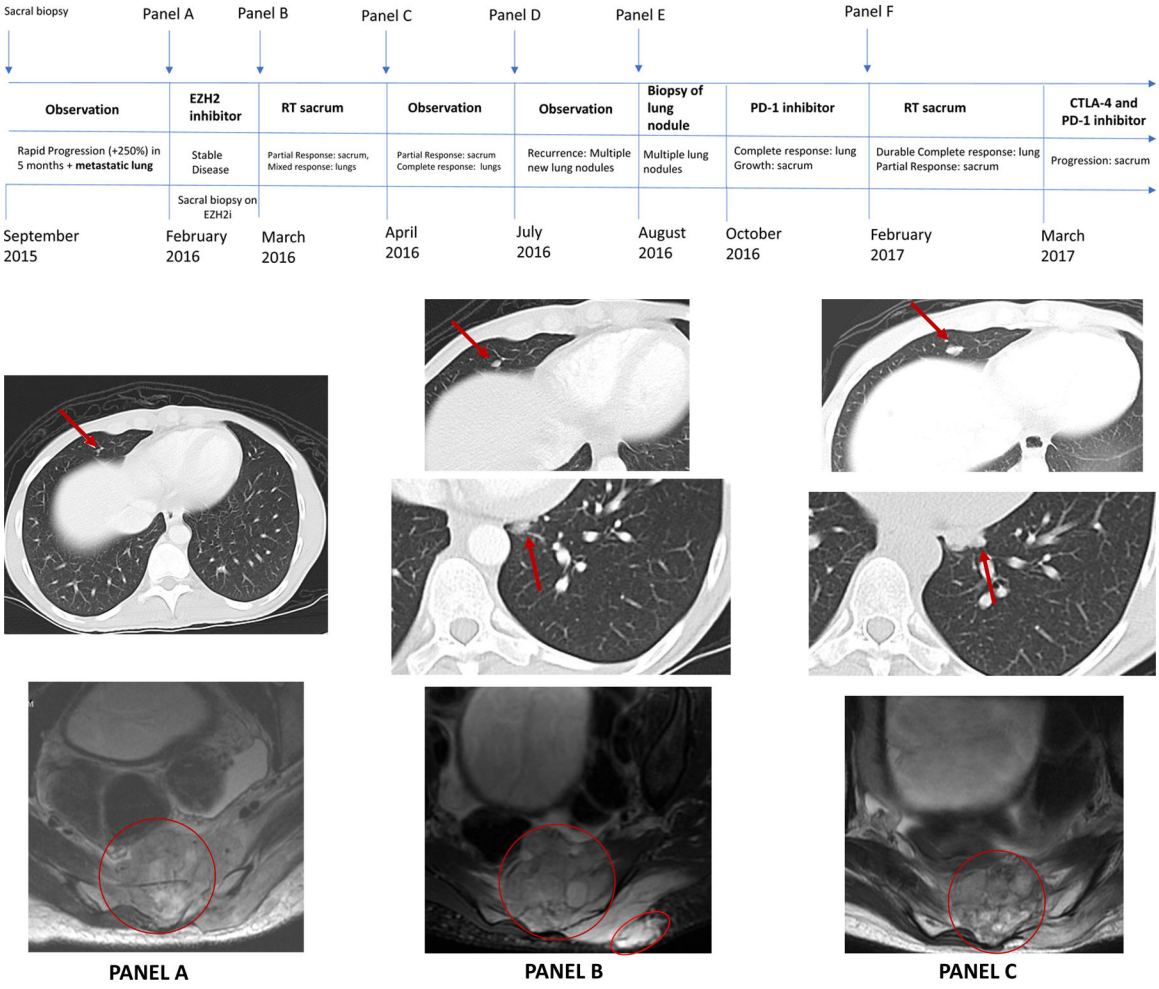

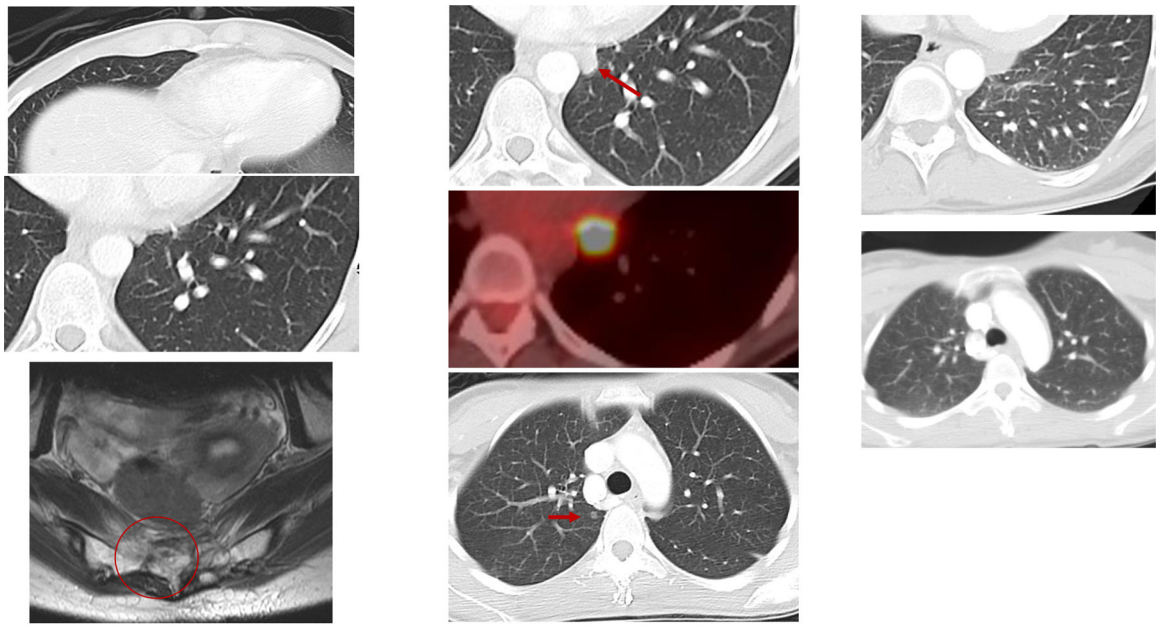

Figure 1: A timeline of events from presentation of symptoms, diagnosis and various treatments.

Panel A: Baseline MRI (February 2016) scan demonstrated a 6.4 × 3.0 cm sacral mass on sagittal T2-weighted images involving S2 – S4 vertebrae, sacral canal and extraosseous involvement of the presacral soft tissues. Staging CT scan demonstrated sub-centimeter mass in the right middle lobe of the lung consistent with metatastic spread.

Panel B: New baseline MRI and CT scan repeated 4 weeks of observation shows a rapidly progressive tumor at local and metastatic site. MRI showed a target lesion measuring 6.1 × 5.7 cm mass on axial T1 (post-contrast) images and CT chest showed further increase in size of the right middle lobe lesion.

Panel C: MRI and CT scan performed after 4 weeks of tazemetostat showed disease stabilization (+13%) by RECIST 1.1.

Panel D: Following radiation to the sacrum (5200 cGy over 26 fractions and 1,800 cGy boost over 9 fractions), an MRI of the primary sacral mass shows partial response in the sacrum and near complete resolution of an extraosseous mass. On CT chest complete response seen in distant, metastatic lung nodules (non-radiated).

Panel E: Four months after completion of tazemetostat and sacral radiation, CT chest showed multiple, bilateral lung nodules with an FDG avid left lower lobe nodule; which was incompletely resected with positive surgical margin.

Panel F: Following initiation of nivolumab, CT scans shows complete response in all distant lung sites that is ongoing (21+ months).

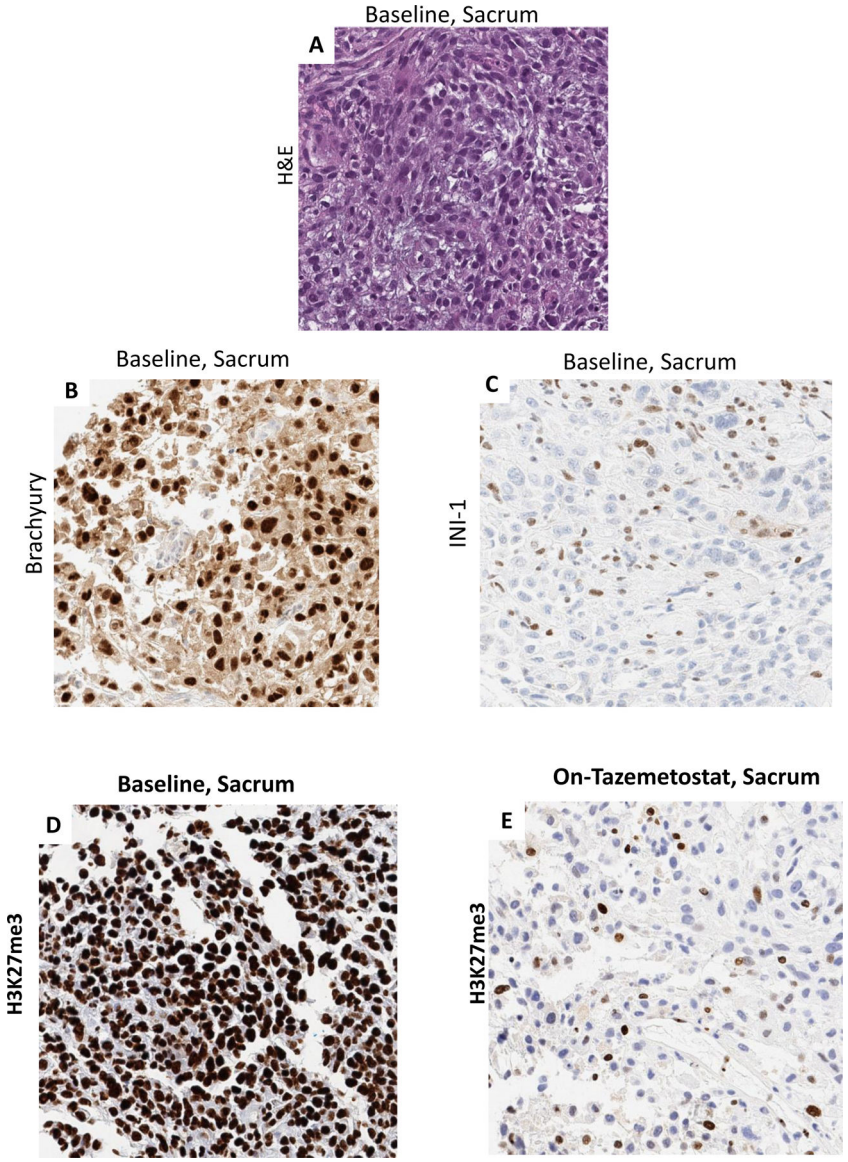

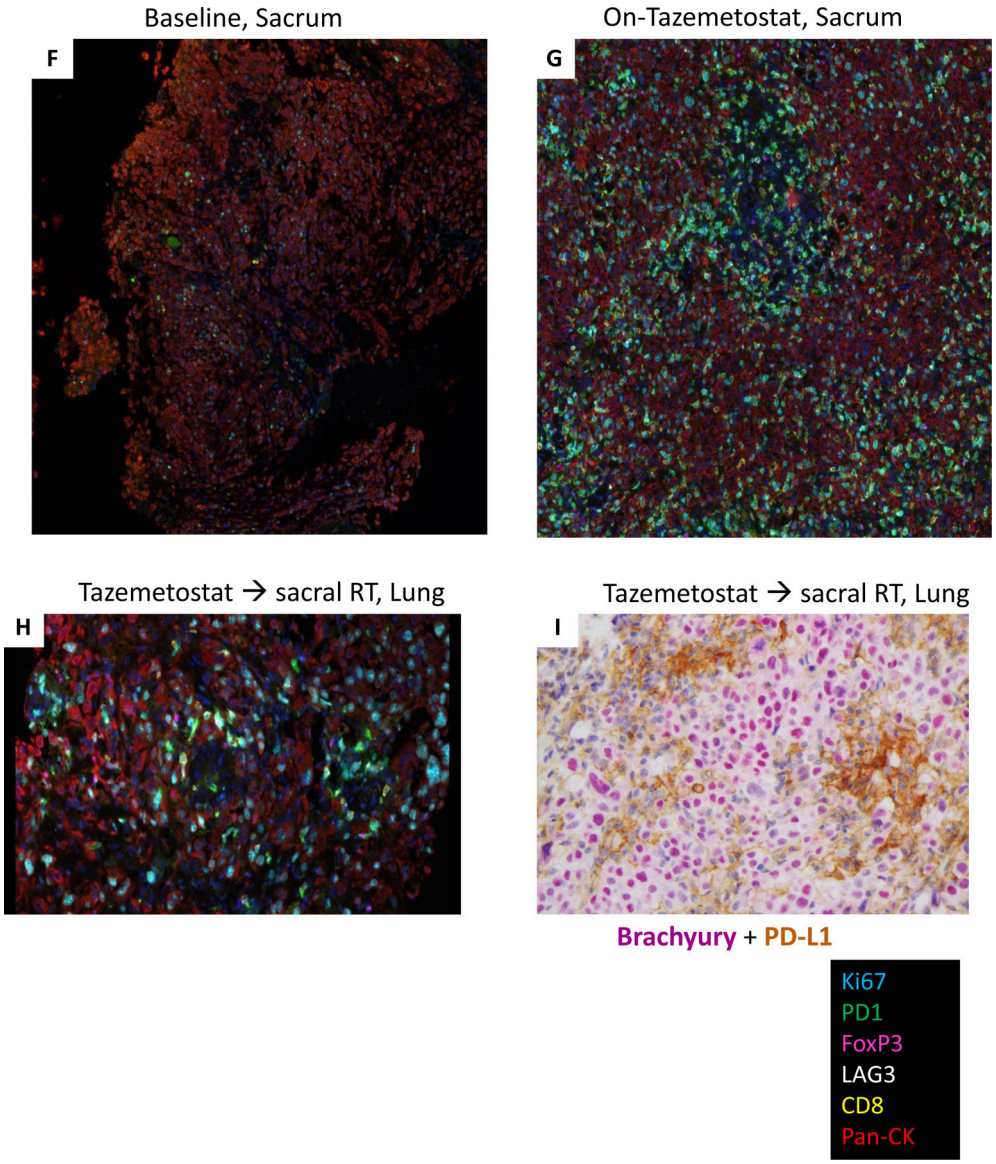

FIGURE 2:

Panel A) Hemotoxylin and Eosin (H&E) stain of primary sacral chordoma shows a cellular neoplasm composed of round to oval cells with abundant clear to eosinophilic cytoplasm, exhibiting moderate to marked nuclear atypia (200X). **Panel B)** immunostain for brachyury – specific for chordoma - showing positive nuclear staining (200X), **Panel C)** INI1 immunostain showing loss of staining in tumor cells (200X). **Panel D)** strong nuclear staining for H3K27me3 is seen at baseline prior to treatment and **Panel E)** near-complete loss of H3K27me3 staining with tazemetostat treatment (200X).

Representative multiplexed fluorescence-based immunostains (Ki67, PD-1, FoxP3, LAG3, CD8, Pan-CK) of the specimens obtained at (**Panel F**) Baseline, sacrum, (**Panel G**) On-tazemetostat, sacrum and (**Panel H**) Tazemetostat followed by radiation, lung. **I**) Representative dual immunohistochemical stain (200x) of the Post-RT and EZH2i, Lung

specimen, demonstrating brachyury expression (nuclear red) in tumor cells and PD-L1 expression (membrane and cytoplasmic-brown) in immune cells.

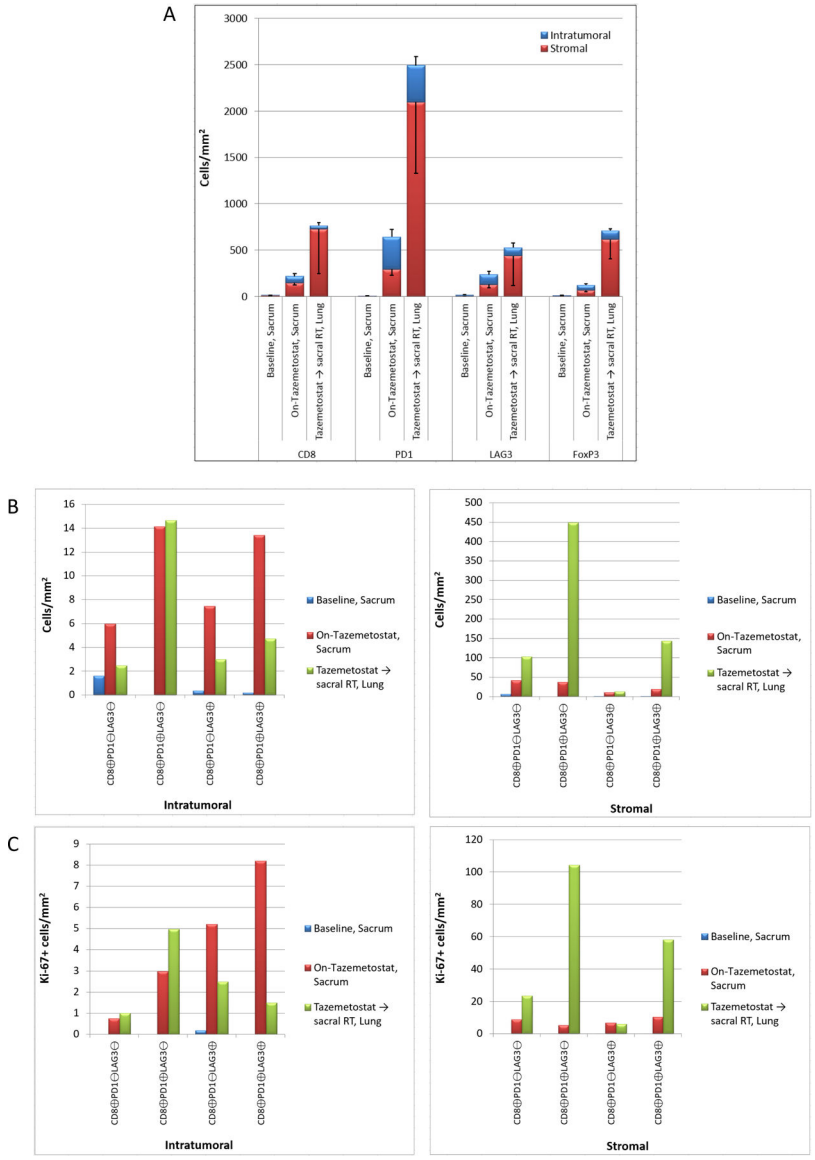

FIGURE 3.

Panel A) Comparison of intratumoral and stromal expression of immune cell markers CD8, PD-1, LAG-3, and FoxP3 in "Baseline, Sacrum", "On-tazemetostat, sacrum", and "Tazemetostat followed by radiation, lung" biopsy samples, quantitated as cells/mm^2. **Panel B)** Comparison of intratumoral (left panel) and stromal (right panel) CD8+ CTL subtypes based on co-expression of PD-1 and LAG-3 in each biopsy, quantitated as cells/mm^2.) **Panel C)** Proliferative indices of CD8+ CTL subtypes based on PD-1 and LAG-3 co-expression (B). The number of intratumoral (left panel) and stromal (right panel) Ki67-positive CD8+ CTL subtypes in each biopsy sample is plotted (cells/mm^2).